Journal of Molecular Spectroscopy 406 (2024) 111953

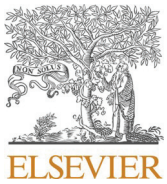

Contents lists available at ScienceDirect

Journal of Molecular Spectroscopy

journal homepage: www.elsevier.com/locate/yjmsp

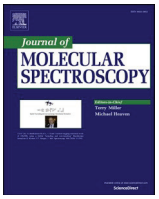

Buffer-gas cooling of hydrogen cyanide quantified by cavity-ringdown spectroscopy

Thomas Howard, Shannon E. Ganley, Sanjana Maheshwari, Leah G. Dodson *

Department of Chemistry and Biochemistry, University of Maryland, College Park, MD 20742, USA

ARTICLE INFO

Keywords:
Buffer-gas cooling
Cavity-ringdown spectroscopy
Overtones
Infrared spectroscopy
Rotational-vibrational spectroscopy
Hydrogen cyanide

ABSTRACT

We describe an instrument that uses continuous-wave (CW) cavity-ringdown spectroscopy to measure the translational and rotational temperature of buffer-gas cooled molecules and demonstrate its use on hydrogen cyanide. This instrument can access the near-infrared region around 1.5 μm—a rich spectral region that features the rotationally resolved first overtone of the C-H stretch for many astrophysically relevant molecules. Molecules are probed directly inside the buffer-gas cell, further enabling quantitative measurements of the effectiveness of this cooling technique.

1. Introduction

Complex organic molecules (COMs) play a central role in the chemistry of the interstellar medium (ISM). These chemical species have been detected in a variety of interstellar and planetary environments and are likely a key ingredient in the formation of prebiotic molecules in space. To aid in molecular detection efforts and the interpretation of astrochemical spectra, laboratory spectroscopic characterization of COMs at high resolution is necessary. Until recently, spectral congestion seriously hindered the spectral analysis of larger (>10 atoms) molecules at any resolution [1]. Buffer-gas cooling offers a solution—a molecule's translational and rotational energy can be reduced through collisions with a cold buffer gas [2], reducing the number of occupied states and simplifying spectral analysis. The spectra can then be characterized in a more straightforward manner with high resolution. Unlike supersonic expansion techniques, buffer-gas cooling generates translationally colder molecules and requires a much lower pressure differential, resulting in greater ease of measurements and less pumping infrastructure [3]. The coupling of buffer-gas cooling with cavity-enhanced spectroscopy techniques allows for the high-resolution and low-noise measurement of cold molecules [4,5]. When compared with single-pass direct-absorption measurements, cavity enhancement enables the measurement of lower concentrations of the molecule of interest or smaller probe volumes—important when dealing with rare, highly reactive, or low-vapor-pressure species.

Cavity-enhanced measurements have been made on buffer-gas cooled molecules such as vinyl bromide [6], acetylene [7], C_{60} [8], and others of atmospheric or astrophysical relevance. In these cases, measurements are made within the buffer-gas cell itself. Acetylene has also been studied using this combination of techniques, but with measurements taken after the molecule exited the buffer-gas cell in the form of a molecular beam [4]. Cavity-ringdown spectroscopy (CRDS) is used in the present work for the collection of high-sensitivity, high-resolution spectral data. CRDS grants us the ability to measure the translational and rotational temperatures of the molecule of interest in the buffer-gas cell, even though that molecule is present at low number density and in a relatively small volume.

In this work we present the design and first results for our cryogenic buffer-gas beam (CBGB) instrument with CRDS detection capabilities passing directly through the buffer-gas cell. A molecular beam is created from the buffer-gas-cooled molecules, which will be used in later trapping and kinetics studies. Hydrogen cyanide (HCN), which has previously been studied at low temperatures in the microwave region using helium nanodroplet isolation [9,10] and buffer-gas cooling [11] is used as a test molecule, due to its well-studied nature in the near-infrared region [12–14], its wide detection in a variety of interstellar environments [15–17], and its significant relevance to many astrochemical models of COM formation in the ISM [18]. CRDS is used to characterize HCN in the buffer-gas cell, and to determine the degree of translational and rotational cooling achieved using the buffer-gas cooling method at temperatures from 300 to 150 K.

* Corresponding author.
E-mail address: ldodson@umd.edu (L.G. Dodson).

https://doi.org/10.1016/j.jms.2024.111953
Received 28 June 2024; Received in revised form 8 October 2024; Accepted 9 October 2024
Available online 11 October 2024

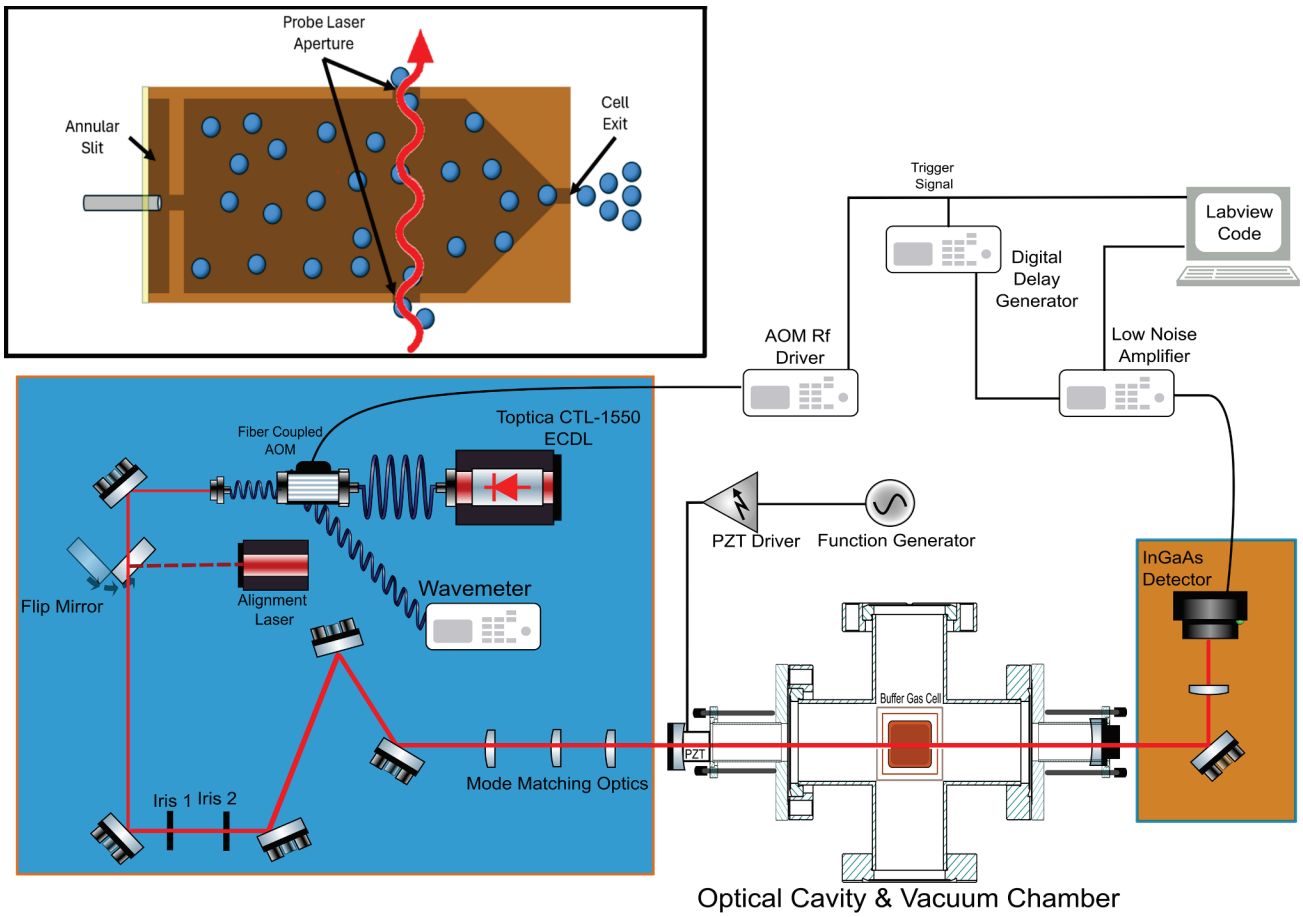

Fig. 1. Block diagram for the CW-CRDS-CBGB spectrometer. The red line traces the path of the near-infrared laser, while black lines indicate electrical connections. The blue and orange sections indicate components that are mounted on optical tables that are not in physical contact with the scaffolding that holds the vacuum chamber. The inset displays a cross sectional view (not to scale) of the geometry of the buffer-gas cell.

2. Experimental methods

Experiments were conducted in a new buffer-gas cooling apparatus equipped with a high-resolution cavity-enhanced detection system (CW-CRDS-CBGB, shown schematically in Fig. 1) at the University of Maryland.

A custom-built buffer-gas cell, based on the planar-conical design of Singh et al. [19] is mounted to the second stage of a closed-cycle helium cryostat (Janis RDK-415D2) that is capable of cooling down to 4 K. The temperature of the buffer-gas cell is maintained by a Lake Shore model 331 temperature controller through the use of a temperature diode and resistive cartridge heater. Gas—composed mostly of helium—flows into the buffer-gas cell through a 0.061″ inner-diameter copper capillary tube and is cooled through collisions with the cold cell walls. The capillary tube is heated above the freezing point of HCN by a second resistive heater. Gases exit the buffer-gas cell through a 0.09″-diameter exit aperture on the conical side opposite from the entrance. The flow of gases through the instrument is maintained by a mass flow controller (Alicat) with an accuracy of 0.05 sccm (1 sccm = 4.5×10^{17} molecules s^{-1}), with typical residence times estimated to range from 2.5 to 15 ms. Holes (0.156″ diameter) are drilled into the side of the cell body approximately 1″ from the cell entrance to admit the laser beam used for spectroscopic measurements. Radiation shielding is attached to the first stage of the cryohead with appropriate apertures to allow gas flow in and out of the buffer-gas cell, as well as laser access. The cold-cell assembly is enclosed within a standard six-way 8″ Conflat cross that is continually pumped by a Leybold 90iX turbomolecular pump. The pressure inside the chamber is typically on the order of 10^{-4} Torr during continuous-flow experiments.

Molecules inside the buffer-gas cell are probed using cavity-ringdown spectroscopy, with the spectroscopic axis perpendicular to the flow axis inside the buffer-gas cell. The 45-cm optical cavity is formed by two high-reflectivity (HR) mirrors (LayerTec, 1550 nm, 99.994 % reflective, 1-m radius-of-curvature, 25 μs theoretical ring-down time) in custom-built optics mounts that are mounted directly to the six-way cross with vibration damping provided by edge-welded bellows tubing. The cavity has a waist of 146 μm and a free spectral range (FSR) of 333 MHz. The probe laser is a tunable diode laser with a linewidth <10 kHz (Toptica CTL-1550) that is chopped by an acousto-optic modulator (Brimrose) that is triggered when a resonant cavity mode reaches a preset threshold voltage and monitored by a wavemeter (Bristol, 228B). The beam is coupled into the optical cavity using a set of three mode-matching lenses and resonance with the cavity is achieved by continuously dithering a cylindrical piezoelectric actuator using a 10-Hz triangle wave. Each ringdown event is collected by an InGaAs biased photodetector (ThorLabs, DET10C2), recorded on a PC oscilloscope (GaGe), and fit with an exponential decay function in a custom data-acquisition program (LabView). The laser is tuned (0.001 nm step size) across an absorption feature and an average of 100 ringdown events is obtained at each wavelength. The absorption coefficient, α, is extracted from the collected ringdown times $\tau(\nu)$ as a function of frequency ν via the following relation (1)

$$\alpha = \frac{L}{dc}\left(\frac{1}{\tau(\nu)} - \frac{1}{\tau_0}\right) \tag{1}$$

where c is the speed of light, $\tau_0 \approx 25$ μs is the ringdown time for an empty

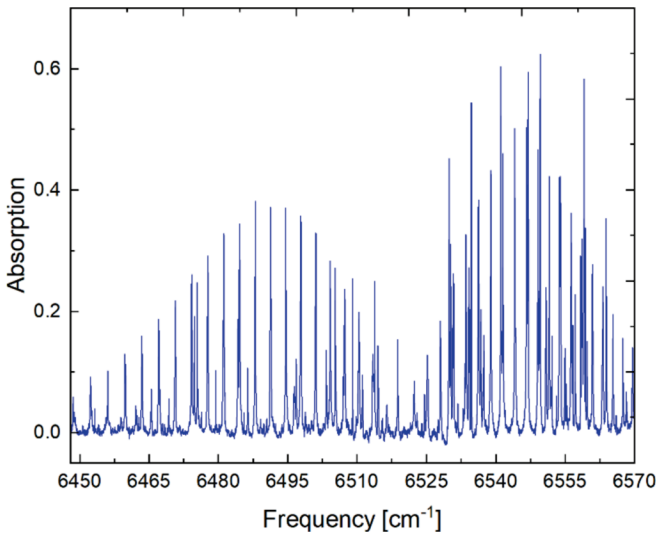

Fig. 2. Room-temperature survey spectrum of the $2\nu_1$ transition of HCN within a portion of the frequency range accessible to our ringdown spectrometer.

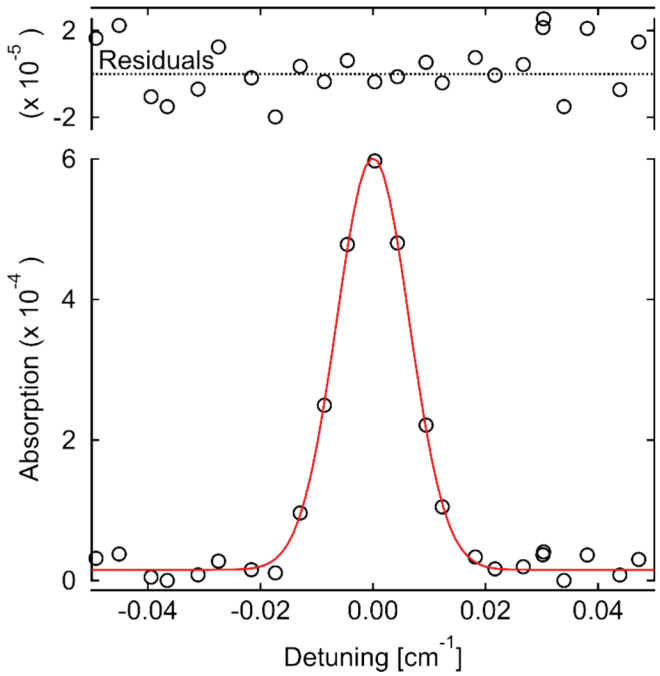

Fig. 3. An example of a fitted rotational-vibrational transition. This shows the P(7) transition for the first overtone of the C-H stretch at 300 K relative to the line center at 6498.03115 cm^{-1}.

cavity, L is the distance between the cavity mirrors, and d is the length of the buffer-gas cell. Reported spectra are the average of three independent data sets.

Hydrogen cyanide was synthesized as described previously [20] by reacting solid KCN with an excess of concentrated H_2SO_4 under active vacuum and condensing/freezing HCN vapors in a liquid nitrogen trap [21]. A stock cylinder was prepared by controlled evaporation of the pure HCN solid with total pressure kept below the vapor pressure of HCN. Custom mixtures of HCN in buffer gas (2 % HCN in ultrahigh-purity helium) were prepared from stock manometrically in sample cylinders. This preparation produces samples that are remarkably free from water or carbon dioxide contamination, as confirmed by gas-phase Fourier-transform infrared spectroscopy.

Table 1
Measured gas-cell temperatures and corresponding observed translational and rotational temperatures of the buffer-gas-cooled HCN (all reported in K).

Gas-Cell Temperature (K)	Translational Temperature (K)	Rotational Temperature (K)
300	290 (±23)	308 (±15)
250	250 (±10)	250 (±21)
200	199 (±2)	220 (±43)
150	147 (±7)	140 (±3)

3. Results and discussion

In these experiments, data were obtained that enabled the measurement of both the translational and rotational temperatures of HCN as a function of buffer-gas cell temperature. While it was possible to measure the entire rotationally resolved $2\nu_1$ C-H stretch overtone band (see Fig. 2), each scan takes about 18 h to complete. Both translational and rotational temperatures could be measured accurately using a smaller range of rotational-vibrational states, which take only about 30 min to complete. We selected the P(1) through P(10) lines of $2\nu_1$ because they are centered in the optimal range for both the high-reflectivity mirrors and the laser. Each peak is identified by comparison to the HITRAN database [22].

Fig. 3 shows a typical spectrum obtained at 300 K from a single scan of the P(7) transition, with discrete data points plotted as black open circles. The data were baseline subtracted and the peak was fit in IgorPro using a Gaussian function (red solid line) and the residuals are plotted above. The peak area and full-width at half-maximum (FWHM) for each peak were evaluated as a function of temperature. The Doppler width was used to obtain the translational temperature by solving for T_{trans} in the formula [23]

$$\frac{FWHM}{2} = \frac{\nu_J}{c}\sqrt{\frac{2N_A k_B T_{trans}}{M}} \tag{2}$$

where ν_J is the center frequency of the rotational transition in cm^{-1}, c is the speed of light in cm s^{-1}, N_A is Avogadro's number, and M is the molar mass of HCN in grams.

We obtained a translational temperature from each fitted peak independently for each set of rotational-vibrational transitions measured at a given buffer-gas cell temperature and computed an average translational temperature. Table 1 reports the FWHM obtained for each rotational-vibrational transition at each cell temperature, along with the computed translational temperature. All fitting parameters and errors are available in Appendix A. The error in T_{trans} comes from the random error in the FWHM obtained from the Gaussian fit. The measured translational temperature is the same as that measured on the buffer-gas cell body to within error for each temperature setting, indicating that the thermal bath in the buffer-gas cell has efficiently cooled the translational motion of HCN.

The HCN rotational temperature (T_{rot}) was obtained using the fitted area for each rotational-vibrational peak in Eq. (3) [24]

$$ln\left(\frac{PeakArea}{\nu_J(J'+J''+1)}\right) = -\frac{E_J}{k_B T_{rot}} \tag{3}$$

where ν_J is the center frequency of the rotational state, J' is the upper value of J for the transition, J'' is the lower value of J, k_B is Boltzmann's constant, T_{rot} is rotational temperature in Kelvin. The lower state energy of the transition E_J (in cm^{-1}) is defined as [25]

$$E_J = \widetilde{B}J''(J''+1) - \widetilde{D}J''^2(J''+1)^2 \tag{4}$$

where $\widetilde{B}$ is the rotational constant and $\widetilde{D}$ is the centrifugal distortion constant for HCN, which are obtained from the NIST Triatomic Spectral Database [26–30]. Plotting $ln\left(\frac{Area}{\nu_J(J'+J''+1)}\right)$ as a function of E_J yields a

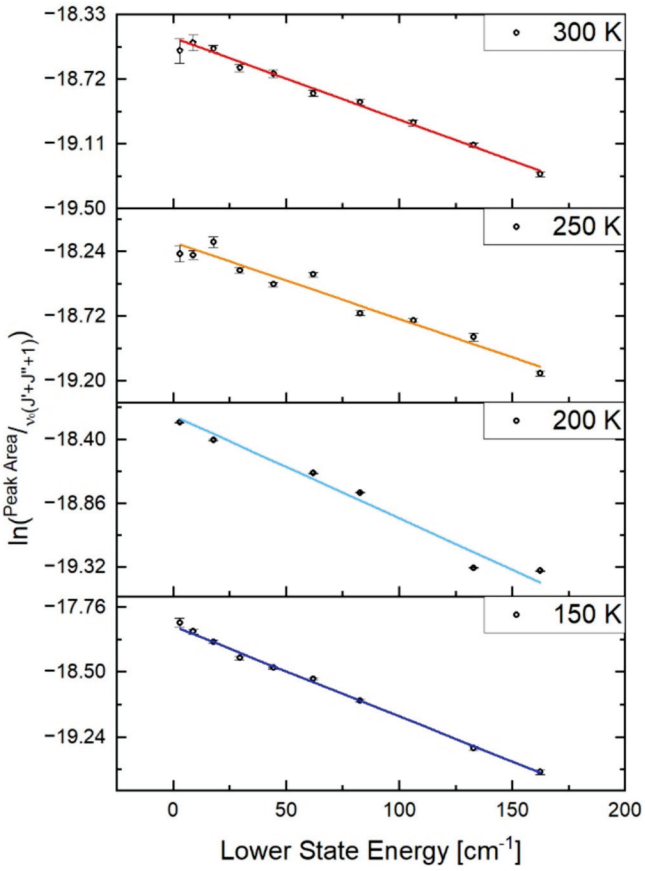

Fig. 4. Boltzmann plot of $2\nu_1$ of HCN at various temperatures. The rotational temperature is calculated using the slope obtained from a linear fit (colored lines) which is equivalent to $-1/k_B T_{\text{rot}}$.

linear "Boltzmann" plot with a slope of $-\frac{1}{k_B T_{\text{rot}}}$, whence the rotational temperature is extracted. Fig. 4 shows the linear dependence from the measured peak areas extracted as a function of lower state energy for several rotational-vibrational transitions, measured at several different cell temperatures. The linear fits for each temperature are shown as solid-colored lines. Table 1 reports the measured T_{rot} for each nominal cell temperature, showing that the rotational degrees of freedom are thermalized—within error—with the cell-wall temperature in all cases except the lowest temperature.

These measurements demonstrate that collisions with buffer-gas helium atoms are effective at cooling both translational and rotational degrees of freedom of HCN. Both translational and rotational measurements match the set temperature of the gas cell within error. Measurement precision could be further increased by improvements to cavity stability and increased number density of the target molecule, as demonstrated by previous buffer-gas cell experiments [4,31]. Although HCN is a volatile species its vapor pressure drops precipitously below 150 K [32] resulting in a large loss of molecules likely due to condensation resulting from gas dynamics within the annular slit. This is further compounded by the fact that it is estimated that only 20 % of target molecules are entrained into the gas cell after leaving the capillary [33]. Modifications to the injection system will avoid this issue and increasing the concentration as cell temperature decreases will mitigate this loss and allow species of interest to be probed at lower temperatures.

4. Conclusions and outlook

We have constructed a new instrument at the University of Maryland capable of preparing cold gaseous molecules by buffer-gas cooling techniques. We have demonstrated the ability to quantify the translational and rotational temperature achieved after cooling the molecule of interest. This technique can be extended to other gas-phase molecules and is a valuable tool to probe low-temperature molecules of astrophysical interest. We showed—using HCN as a prototypical molecule—that the temperature of the cold cell equals the temperature of the molecule down to cold-cell temperatures of 150 K. While the cold cell can be cooled to temperatures as low as 15 K, the temperature lower limit for the present study was the result of poor gas dynamics in the annular slit compounded by the HCN vapor pressure dropping dramatically near 150 K [32], resulting in the HCN concentration dropping below our sensitivity limit. In the future, the sensitivity of this instrument can be further improved by refining the method by which molecules are injected into the buffer-gas cell and implementing an active cavity locking system—such as the Pound-Drever-Hall scheme—potentially enabling measurements to be made at lower temperatures.

CRediT authorship contribution statement

Thomas Howard: Writing – original draft, Visualization, Software, Methodology, Investigation, Formal analysis, Data curation. **Shannon E. Ganley:** Writing – original draft, Visualization, Software, Investigation, Formal analysis. **Sanjana Maheshwari:** Writing – review & editing, Investigation. **Leah G. Dodson:** Writing – review & editing, Supervision, Resources, Funding acquisition, Conceptualization.

Declaration of competing interest

The authors declare the following financial interests/personal relationships which may be considered as potential competing interests: Corresponding author is a member of the Journal of Molecular Spectroscopy editorial board. If there are other authors, they declare that they have no known competing financial interests or personal relationships that could have appeared to influence the work reported in this paper.

Acknowledgements

This material is based upon work supported by the National Science Foundation under Grant No. 2154055. Additional support for this work was provided by a University of Maryland startup grant. Acknowledgment is made to the Optical Measurements Group (NIST) for guidance in creating the data acquisition and fitting program. We are grateful to Kevin Lehmann (UVA) for loaning initial equipment.

Appendix A. Supplementary data

Supplementary data to this article can be found online at https://doi.org/10.1016/j.jms.2024.111953.

Data availability

Data will be made available on request.

References

[1] J.P. Porterfield, L. Satterthwaite, S. Eibenberger, D. Patterson, M.C. McCarthy, High sensitivity microwave spectroscopy in a cryogenic buffer gas cell, Rev. Sci. Instrum. 90 (5) (2019) 053104, https://doi.org/10.1063/1.5091773.
[2] J.K. Messer, F.C. De Lucia, Measurement of pressure-broadening parameters for the CO-He system at 4 K, Phys. Rev. Lett. 53 (27) (1984) 2555–2558, https://doi.org/10.1103/PhysRevLett.53.2555.
[3] N.R. Hutzler, H.-I. Lu, J.M. Doyle, The buffer gas beam: an intense, cold, and slow source for atoms and molecules, Chem. Rev. 112 (9) (2012) 4803–4827, https://doi.org/10.1021/cr200362u.
[4] L. Santamaria, V. Di Sarno, P. De Natale, M. De Rosa, M. Inguscio, S. Mosca, I. Ricciardi, D. Calonico, F. Levi, P. Maddaloni, Comb-assisted cavity ring-down spectroscopy of a buffer-gas-cooled molecular beam, Phys. Chem. Chem. Phys. 18 (25) (2016) 16715–16720, https://doi.org/10.1039/C6CP02163H.

[5] B. Spaun, P.B. Changala, D. Patterson, B.J. Bjork, O.H. Heckl, J.M. Doyle, J. Ye, Continuous probing of cold complex molecules with infrared frequency comb spectroscopy, Nature 533 (7604) (2016) 517–520, https://doi.org/10.1038/nature17440.
[6] P.B. Changala, B. Spaun, D. Patterson, J.M. Doyle, J. Ye, Sensitivity and resolution in frequency comb spectroscopy of buffer gas cooled polyatomic molecules, in: D. Meschede, T. Udem, T. Esslinger (Eds.), Exploring the World with the Laser: Dedicated to Theodor Hänsch on his 75th birthday, Springer International Publishing, Cham, 2018, pp. 647–664, https://doi.org/10.1007/978-3-319-64346-5_35.
[7] V.D. Sarno, R. Aiello, M.D. Rosa, I. Ricciardi, S. Mosca, G. Notariale, P.D. Natale, L. Santamaria, P. Maddaloni, Lamb-dip spectroscopy of buffer-gas-cooled molecules, Optica 6 (4) (2019) 436–441, https://doi.org/10.1364/OPTICA.6.000436.
[8] P.B. Changala, M.L. Weichman, K.F. Lee, M.E. Fermann, J. Ye, Rovibrational quantum state resolution of the C_{60} fullerene, Science 363 (6422) (2019) 49–54, https://doi.org/10.1126/science.aav2616.
[9] C. Callegari, A. Conjusteau, I. Reinhard, K.K. Lehmann, G. Scoles, First overtone helium nanodroplet isolation spectroscopy of molecules bearing the acetylenic CH chromophore, J. Chem. Phys. 113 (23) (2000) 10535–10550, https://doi.org/10.1063/1.1324003.
[10] A. Conjusteau, C. Callegari, I. Reinhard, K.K. Lehmann, G. Scoles, Microwave spectra of HCN and DCN in ^{4}He nanodroplets: A test of adiabatic following, J. Chem. Phys. 113 (12) (2000) 4840–4843, https://doi.org/10.1063/1.1310603.
[11] T.J. Ronningen, F.C. De Lucia, Helium induced pressure broadening and shifting of HCN hyperfine transitions between 1.3 and 20 K, J. Chem. Phys. 122 (18) (2005) 184319, https://doi.org/10.1063/1.1895905.
[12] H. Sasada, K. Yamada, Calibration lines of HCN in the 1.5-μm region, Appl. Opt. 29 (24) (1990) 3535–3547, https://doi.org/10.1364/AO.29.003535.
[13] W.C. Swann, S.L. Gilbert, Line centers, pressure shift, and pressure broadening of 1530–1560 nm hydrogen cyanide wavelength calibration lines, JOSA B 22 (8) (2005) 1749–1756, https://doi.org/10.1364/JOSAB.22.001749.
[14] G.C. Mellau, B.P. Winnewisser, M. Winnewisser, Near infrared emission spectrum of HCN, J. Mol. Spectrosc. 249 (1) (2008) 23–42, https://doi.org/10.1016/j.jms.2008.01.006.
[15] A. Adriani, B.M. Dinelli, M. López-Puertas, M. García-Comas, M.L. Moriconi, E. D'Aversa, B. Funke, A. Coradini, Distribution of HCN in Titan's upper atmosphere from Cassini/VIMS observations at 3 μm, Icarus 214 (2) (2011) 584–595, https://doi.org/10.1016/j.icarus.2011.04.016.
[16] T.M. Dame, C.J. Lada, A complete HCN survey of the Perseus molecular cloud, Astrophys. J. 944 (2) (2023) 197, https://doi.org/10.3847/1538-4357/acb438.
[17] W.F. Huebner, L.E. Snyder, D. Buhl, HCN radio emission from Comet Kohoutek (1973f), Icarus 23 (4) (1974) 580–584, https://doi.org/10.1016/0019-1035(74)90023-2.
[18] S.H. Jung, J.C. Choe, Mechanisms of prebiotic adenine synthesis from HCN by oligomerization in the gas phase, Astrobiology 13 (5) (2013) 465–475, https://doi.org/10.1089/ast.2013.0973.
[19] V. Singh, A.K. Samanta, N. Roth, D. Gusa, T. Ossenbrüggen, I. Rubinsky, D. A. Horke, J. Küpper, Optimized cell geometry for buffer-gas-cooled molecular-beam sources, Phys. Rev. A 97 (3) (2018) 032704, https://doi.org/10.1103/PhysRevA.97.032704.
[20] E.K. Hockey, K. Vlahos, T. Howard, J. Palko, L.G. Dodson, Weakly bound complex formation between HCN and CH_3Cl: a matrix-isolation and computational study, J. Phys. Chem. A 126 (20) (2022) 3110–3123, https://doi.org/10.1021/acs.jpca.2c00716.
[21] Hydrogen Cyanide (Anhydrous), Org. Synth. 7 (1927) 50. doi: 10.15227/orgsyn.007.0050.
[22] *The HITRAN2020 molecular spectroscopic database - ScienceDirect.* https://www.sciencedirect.com/science/article/pii/S0022407321004416?via%3Dihub (accessed 2024-05-14).
[23] P.F. Bernath, Spectra of Atoms and Molecules, Oxford University Press, 2005.
[24] G. Herzberg, Molecular Spectra and Molecular Structure: Spectra of Diatomic Molecules, Van Nostrand, 1950.
[25] P.W. Atkins, J. De Paula, J. Keeler, Atkins' Physical Chemistry, eleventh ed., Oxford University Press, Oxford, United Kingdom, 2018.
[26] Triatomic Spectral Database. *NIST,* **2009**.
[27] A.G. Maki, Microwave spectra of molecules of astrophysical interest VI. Carbonyl sulfide and hydrogen cyanide, J. Phys. Chem. Ref. Data 3 (1) (1974) 221–244, https://doi.org/10.1063/1.3253139.
[28] A.G. Maki Jr., D.R. Lide Jr., Microwave and Infrared Measurements on HCN and DCN: Observations on *l*-Type Resonance Doublets, J. Chem. Phys. 47 (9) (1967) 3206–3210, https://doi.org/10.1063/1.1712376.
[29] G. Winnewisser, A.G. Maki, D.R. Johnson, Rotational constants for HCN and DCN, J. Mol. Spectrosc. 39 (1) (1971) 149–158, https://doi.org/10.1016/0022-2852(71)90286-4.
[30] T. Törring, l-Typ-Dubletts der isotopen HCN-Molekeln, Z. Für Phys. 161 (2) (1961) 179–189, https://doi.org/10.1007/BF01332444.
[31] L. Santamaria, V.D. Sarno, I. Ricciardi, M.D. Rosa, S. Mosca, G. Santambrogio, P. Maddaloni, P.D. Natale, Low-temperature spectroscopy of the $^{12}C_2H_2$ ($\nu_1 + \nu_3$) band in a helium buffer gas, Astrophys. J. 801 (1) (2015) 50, https://doi.org/10.1088/0004-637X/801/1/50.
[32] R.L. Hudson, P.A. Gerakines, Infrared spectra and vapor pressures of crystalline C_2N_2, with comparisons to crystalline HCN, Planet. Sci. J. 4 (11) (2023) 205, https://doi.org/10.3847/PSJ/ad0040.
[33] D. Patterson, J.M. Doyle, Cooling molecules in a cell for FTMW spectroscopy, Mol. Phys. 110 (15–16) (2012) 1757–1766, https://doi.org/10.1080/00268976.2012.679632.